

NUMERICAL METHODS FOR DIFFERENTIAL EQUATIONS IN RANDOM DOMAINS*

DONGBIN XIU[†] AND DANIEL M. TARTAKOVSKY[‡]

Abstract. Physical phenomena in domains with rough boundaries play an important role in a variety of applications. Often the topology of such boundaries cannot be accurately described in all of its relevant detail due to either insufficient data or measurement errors or both. This topological uncertainty can be efficiently handled by treating rough boundaries as random fields, so that an underlying physical phenomenon is described by deterministic or stochastic differential equations in random domains. To deal with this class of problems, we propose a novel computational framework, which is based on using stochastic mappings to transform the original *deterministic/stochastic problem in a random domain* into a *stochastic problem in a deterministic domain*. The latter problem has been studied more extensively, and existing analytical/numerical techniques can be readily applied. In this paper, we employ both a stochastic Galerkin method and Monte Carlo simulations to solve the transformed stochastic problem. We demonstrate our approach by applying it to an elliptic problem in single- and double-connected random domains, and comment on the accuracy and convergence of the numerical methods.

Key words. random domain, stochastic inputs, differential equations, uncertainty quantification

AMS subject classifications. 60H15, 60H35, 65C20, 65C30

DOI. 10.1137/040613160

1. Introduction. Physical phenomena described by differential equations in domains with rough geometries are ubiquitous and include applications ranging from surface imaging [24] to manufacturing of nano-devices [5]. Indeed, given a proper spatial resolution, virtually any natural or manufactured surface becomes rough. Consequently, there is a growing interest in experimental, theoretical, and numerical studies of deterministic and probabilistic descriptions of such surfaces and of solutions of differential equations defined on the resulting domains.

The early attempts to represent surface roughness and to study its effects on system behavior were based on simplified, easily parameterizable, *deterministic* surface inhomogeneities, such as symmetrical asperities to represent indentations [32, 26] and semispheres to represent protrusions [17]. More general representations of surface roughness, which nevertheless admit simple parameterizations, include sinusoidal corrugations [13] and periodic linear segments [6]. A recent trend in describing surface roughness is to use fractal and fractal-like representation. These include deterministic Von Koch's [10, 6, 8] and Minkowski's [6] fractals, as well as their random generalizations [29].

*Received by the editors August 9, 2004; accepted for publication (in revised form) February 7, 2006; published electronically July 17, 2006.

<http://www.siam.org/journals/sisc/28-3/61316.html>

[†]Department of Mathematics, Purdue University, West Lafayette, IN 47907 (dxiu@math.purdue.edu).

[‡]Department of Mechanical and Aerospace Engineering, the University of California, San Diego, La Jolla, CA 92093, and Theoretical Division, Los Alamos National Laboratory, Los Alamos, NM 87545 (dmt@ucsd.edu). The work of this author was performed at Los Alamos National Laboratory (LA-UR 04-5497) under the auspices of the National Nuclear Security Agency of the U.S. Department of Energy under contract W-7405-ENG-36 and was supported in part by the U.S. Department of Energy under the DOE/BES Program in the Applied Mathematical Sciences, contract KC-07-01-01, and in part by the LDRD Program at Los Alamos National Laboratory.

Alternatively, one can use *random* fields to represent rough surfaces whose detailed topology cannot be ascertained due to the lack of sufficient information and/or measurement errors [15, 27]. In this paper, we adopt random representations of rough surfaces, because of their generality. Such an approach allows us not only to make predictions of the system behavior, but also to quantify the corresponding predictive uncertainties.

The presence of uncertainty in rough boundaries necessitates the development of new approaches for the analysis and numerical solution of differential equations defined on random domains. For example, classical variational formulations might not be suitable for such problems [1], and a finite difference approach [34] is shown to be accurate only for relatively simple rectangular irregularities. Most of the existing analyses deal with deterministic roughness and are very problem-specific. For example, the use of conformal mappings [7, 6] requires that a physical phenomenon be accurately described by Laplace's equation in two dimensions, while the use of the Liebmann method [8] requires a particular geometry configuration and Dirichlet boundary conditions on the rough surface.

Adoption of a probabilistic framework to describe rough surfaces renders even essentially deterministic problems stochastic; e.g., deterministic equations in random domains give rise to stochastic boundary-value problems. This necessitates the search for new stochastic analyses and algorithms. For example, rigorous bounds for elliptic problems on random domains have been derived for both Dirichlet [2] and Neumann [1] boundary conditions, and perturbation solutions of Laplace's equation in a domain bounded by a random fractal boundary with a small surface dimension have been obtained [29]. One of the very few existing numerical studies employed traditional Monte Carlo simulations [6], which turned out to be so computationally expensive as to become impractical.

In this paper, we present a computational framework that is applicable to a wide class of deterministic and stochastic differential equations defined on domains with random (rough) boundaries. A key component of this framework is the use of robust stochastic mappings to transform an original deterministic or stochastic differential equation defined on a *random domain* into a stochastic differential equation defined on a *deterministic domain*. This allows us to employ the well-developed theoretical and numerical techniques for solving stochastic differential equations in deterministic domains. The idea of transforming irregular domains into their regular counterparts has been used in computational fluid dynamics [33] and optimization problems [4], among other applications. The proposed approach extends this idea to stochastic problems.

In section 2, we provide a general mathematical formulation of a random domain problem. A stochastic mapping technique, which is defined by a solution of an appropriate boundary value problem for Laplace's equation, is presented in section 3.2. A mathematical formulation of the transformed stochastic equations in deterministic domains is given in section 3.3. This section also contains the description of two numerical approaches, Monte Carlo simulations (section 3.3.1) and a stochastic Galerkin method (section 3.3.2), whose relative strengths are discussed in section 3.3.3. In section 4, we apply our computational approach to a two-dimensional elliptic problem defined on both single- and double-connected random domains. For moderately high random dimensions (up to 16-dimensional random space), the stochastic Galerkin method is shown to be more efficient than Monte Carlo simulations. We conclude by listing a few open issues in section 5.

2. Differential equations in random domains. Let $\omega \in \Omega$ be a random realization drawn from a complete probability space $(\Omega, \mathcal{A}, \mathcal{P})$, whose event space Ω generates its σ -algebra $\mathcal{A} \subset 2^\Omega$ and is characterized by a probability measure \mathcal{P} . For all $\omega \in \Omega$, let $D(\omega) \subset \mathbb{R}^d$ be a d -dimensional random domain ($d = 1, 2, 3$), bounded by boundary $\partial D(\omega)$, some or all of whose segments are random. We consider the following stochastic (linear or nonlinear) boundary value problem: for \mathcal{P} -almost everywhere (a.e.) in Ω , given $a : D(\omega) \rightarrow \mathbb{R}$ and $b : \partial D(\omega) \rightarrow \mathbb{R}$, find a stochastic solution $v : \bar{D}(\omega) \rightarrow \mathbb{R}$ such that

$$(2.1) \quad \begin{aligned} L(x; v) &= a(x) && \text{in } D(\omega), \\ B(x; v) &= b(x) && \text{on } \partial D(\omega). \end{aligned}$$

Here $x = (x_1, \dots, x_d)$ is the coordinate in \mathbb{R}^d , L is a differential operator, and B is a boundary operator. The operator B can take various forms on different boundary segments, e.g., $B \equiv I$, where I is the identity operator, on Dirichlet segments and $B \equiv \mathbf{n} \cdot \nabla$ on Neumann segments whose outward unit normal vector is \mathbf{n} . The operators L and B , as well as the driving terms a and b , can be either deterministic or random. To simplify the presentation, we assume that the shape of the boundary $\partial D(\omega)$ is the only source of randomness. This is done without loss of generality, since incorporation of other sources of randomness is straightforward, and stochastic equations in deterministic domains have been studied extensively. Finally, we assume that the random boundary $\partial D(\omega)$ is sufficiently regular, and the boundary condition in (2.1) is properly posed, to guarantee the well-posedness a.e. $\omega \in \Omega$ of the stochastic boundary-value problem (SBVP) (2.1). We refer to this problem as a random domain problem or RDP.

Except for a few studies mentioned in section 1, and despite their practical and theoretical importance, RDPs have not been systematically analyzed. At the same time, the theory of stochastic partial differential equations in fixed deterministic domains is relatively mature. To take advantage of the existing methods for deterministic domains, we introduce a one-to-one mapping function and its inverse

$$(2.2) \quad \xi = \xi(x, \omega), \quad x = x(\xi, \omega),$$

which transforms the random domain $D(\omega) \subset \mathbb{R}^d$ into a deterministic domain $E \subset \mathbb{R}^d$, whose coordinates are denoted as $\xi = (\xi_1, \dots, \xi_d)$; i.e., for \mathcal{P} -a.e. $\omega \in \Omega$,

$$(2.3) \quad x \in D(\omega) \longleftrightarrow \xi \in E.$$

The stochastic mapping (2.3) transforms the deterministic differential operators L and B into their stochastic counterparts \mathcal{L} and \mathcal{B} , respectively, and RDP (2.1) into the following SBVP. For \mathcal{P} -a.e. $\omega \in \Omega$, given $f : E \times \Omega \rightarrow \mathbb{R}$ and $g : \partial E \times \Omega \rightarrow \mathbb{R}$, find a stochastic solution $u : \bar{E} \times \Omega \rightarrow \mathbb{R}$ such that

$$(2.4) \quad \begin{aligned} \mathcal{L}(\xi, \omega; u) &= f(\xi, \omega) && \text{in } E, \\ \mathcal{B}(\xi, \omega; u) &= g(\xi, \omega) && \text{on } \partial E, \end{aligned}$$

where f and g are the transformed functions of a and b , respectively. Note that since the random mapping (2.3) depends *only* on random $D(\omega)$, other possible sources of randomness, including coefficients of the differential operators in (2.1) and boundary and initial conditions, can be easily incorporated into the formulation of RDP (2.1) and do not change the following analysis.

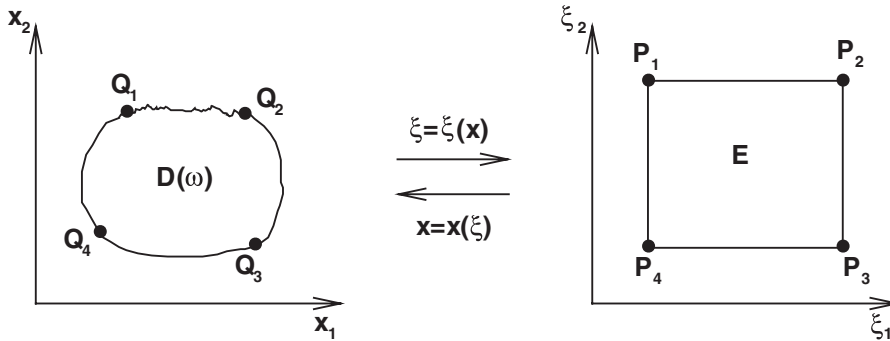


FIG. 2.1. A schematic representation of a computational domain $D(\omega)$ with the random boundary segment $\widehat{Q_1Q_2}$ and its mapping onto a deterministic rectangular domain E , where four reference points Q_i are mapped onto P_i , $i = 1, 2, 3, 4$.

The geometry of the deterministic domain E is to a large extent arbitrary and should be chosen in a way that simplifies the subsequent analysis and computation. Consider, for example, the domain $D(\omega)$ in Figure 2.1, whose boundary segment $\widehat{Q_1Q_2}(\omega)$ is random. Possible choices of the corresponding deterministic domain E include domains whose deterministic boundary segments remain unchanged, and the random boundary segment $\widehat{Q_1Q_2}(\omega)$ is replaced with (i) its ensemble mean $\mathbb{E}[\widehat{Q_1Q_2}(\omega)]$, where \mathbb{E} denotes the expectation operator in the probability space, and (ii) its upper or lower bounds. (Depending on the problem, one can define such bounds based on either the total volume of $D(\omega)$ or the distance of $\partial D(\omega)$ to a certain location in the domain of interest, or in some other way.) Here, to facilitate numerical simulations in the transformed domain E , we choose it to have a canonical shape, such as the rectangle $\widehat{P_1P_2P_3P_4}$ shown in Figure 2.1.

3. Computational framework. A computational framework that is applicable to a wide range of practical applications should provide (i) a general parameterization of the random boundary $\partial D(\omega)$, (ii) an effective way to obtain the stochastic mapping (2.2), and (iii) an efficient method for solving the subsequent SBVP (2.4) in deterministic domains. We construct such a framework by introducing a stochastic mapping based on solutions of Laplace's equations (section 3.2), and by employing two complementary numerical algorithms to solve the resulting SBVPs: a Monte Carlo method and a stochastic Galerkin method (section 3.3).

While the approach discussed in this section is applicable to one- and three-dimensional problems as well, here we consider the two-dimensional domain shown in Figure 2.1, to simplify the presentation. Without loss of generality, we assume that only the segment $\widehat{Q_1Q_2}$ of the overall boundary $\partial D(\omega)$ is random, and we represent it as $\widehat{Q_1Q_2}(\omega) = r(z, \omega)\mathbf{e}_1 + s(z, \omega)\mathbf{e}_2$, where \mathbf{e}_1 and \mathbf{e}_2 are unit vectors in the x_1 and x_2 directions, respectively; r and s are the parameterization functions for the segment; and z is the parameterization variable. We seek to map $D(\omega)$ onto a square $E = [0, 1] \times [0, 1]$.

3.1. Parameterization of random boundary. Parameterization of the random boundary $\widehat{Q_1Q_2}$ consists of the following steps. First, we use Reynolds decomposition to represent random functions, e.g., $A(\omega) = \langle A \rangle + A'(\omega)$, as the sums of

their ensemble means $\langle A \rangle \equiv \mathbb{E}[A(\omega)]$ and zero-mean fluctuations $A'(\omega)$. The latter term can be characterized by a variety of techniques, including its representation as a random field with a given point distribution and two-point correlation function. Here, following common practice, we approximate the fluctuation term by a finite number $K \geq 1$ of mutually uncorrelated random variables $Y_1(\omega), \dots, Y_K(\omega)$ with zero mean and unit variance, so that $r(z, \omega)$ and $s(z, \omega)$ in (3.4) can be approximated as

$$(3.1) \quad r(z, \omega) \approx \langle r(z) \rangle + \sum_{k=1}^K \hat{r}_k(z) Y_k(\omega)$$

and

$$(3.2) \quad s(z, \omega) \approx \langle s(z) \rangle + \sum_{k=1}^K \hat{s}_k(z) Y_k(\omega).$$

The parameterization (3.1) and (3.2) is an approximation of the true processes, whose accuracy and robustness are the subject of ongoing research in the field of numerical generation of random processes. If these processes are non-Gaussian, this task becomes particularly challenging [16, 28, 30, 39]. (In such cases, the goal is often reduced to approximating pointwise marginal distribution functions and two-point covariance functions.) Analysis of the errors induced by the finite-term representations in (3.1) and (3.2), as well as of their efficiency, is beyond the scope of this paper. Instead we refer the interested reader to the references mentioned above.

The choice of a parameterization of the random boundary $\widehat{Q_1 Q_2}$ defines the expansion coefficients $\{\hat{r}_k\}$ and $\{\hat{s}_k\}$. One popular choice is the Karhunen–Loève (KL) decomposition [23], which is an optimal decomposition in terms of the mean-square approximation error and has been used extensively to represent random inputs [3, 14, 36]. Other types of decomposition also can be employed. In section 4 of this paper, we explore both the KL expansion and a Fourier expansion.

3.2. Mapping of the random domain. We construct the stochastic mapping of $D(\omega)$ onto E via solutions of the Laplace equations

$$(3.3) \quad \frac{\partial^2 x_1}{\partial \xi_1^2} + \frac{\partial^2 x_1}{\partial \xi_2^2} = 0, \quad \frac{\partial^2 x_2}{\partial \xi_1^2} + \frac{\partial^2 x_2}{\partial \xi_2^2} = 0 \quad \text{in } E,$$

subject to the boundary conditions

$$(3.4a) \quad x_1(0, \xi_2) = x_1|_{\widehat{Q_4 Q_1}}, \quad x_1(1, \xi_2) = x_1|_{\widehat{Q_3 Q_2}},$$

$$(3.4b) \quad x_1(\xi_1, 0) = x_1|_{\widehat{Q_4 Q_3}}, \quad x_1(\xi_1, 1) = r(z, \omega)$$

and

$$(3.4c) \quad x_2(0, \xi_2) = x_2|_{\widehat{Q_4 Q_1}}, \quad x_2(1, \xi_2) = x_2|_{\widehat{Q_3 Q_2}},$$

$$(3.4d) \quad x_2(\xi_1, 0) = x_2|_{\widehat{Q_4 Q_3}}, \quad x_2(\xi_1, 1) = s(z, \omega),$$

where $x_i|_{\widehat{Q_m Q_n}}$ denotes the x_i coordinate along the boundary segment $\widehat{Q_m Q_n}$. Similar mappings have been used extensively to solve numerically deterministic problems in structured body-fitted curvilinear coordinates [33], and more recently to analyze the interface dynamics in disordered media [19]. The properties and a more detailed

technical description of such mappings can be found in [33]. The stochastic mapping (3.3)–(3.4) can be viewed as a generalization of this idea to random domains. We also remark that the boundary conditions (3.4) are not expressed in a definitive manner. One can choose different distributions of boundary coordinates in x as boundary conditions in (3.4), in order to achieve better computational results by, e.g., clustering a mesh close to the regions of interests (see [33] for details).

As a result of (3.1) and (3.2), solutions of (3.3) can be expressed as

$$(3.5) \quad x_i(\xi, \omega) = \sum_{k=0}^K \hat{x}_{i,k} Y_k(\omega), \quad i = 1, 2.$$

Then, denoting $\hat{r}_0 \equiv \langle r \rangle$ and $\hat{s}_0 \equiv \langle s \rangle$, substituting the expansions (3.1) and (3.5) into (3.3)–(3.4), and collecting the terms of each $\{Y_k(\omega)\}$, i.e., conducting a Galerkin projection (in the random space) of the resulting equations onto the basis spanned by $\{1, Y_1(\omega), \dots, Y_K(\omega)\}$, we obtain $(K + 1)$ equations for the expansion coefficients,

$$(3.6) \quad \frac{\partial^2 \hat{x}_{1,k}}{\partial \xi_1^2} + \frac{\partial^2 \hat{x}_{1,k}}{\partial \xi_2^2} = 0, \quad \frac{\partial^2 \hat{x}_{2,k}}{\partial \xi_1^2} + \frac{\partial^2 \hat{x}_{2,k}}{\partial \xi_2^2} = 0, \quad k = 0, \dots, K,$$

subject to the boundary conditions

$$(3.7a) \quad \hat{x}_{1,k}(0, \xi_2) = x_1|_{\widehat{Q_4 Q_1}} \cdot \delta_{k0}, \quad \hat{x}_{1,k}(1, \xi_2) = x_1|_{\widehat{Q_3 Q_2}} \cdot \delta_{k0},$$

$$(3.7b) \quad \hat{x}_{1,k}(\xi_1, 0) = x_1|_{\widehat{Q_4 Q_3}} \cdot \delta_{k0}, \quad \hat{x}_{1,k}(\xi_1, 1) = \hat{r}_k(z)$$

and

$$(3.7c) \quad \hat{x}_{2,k}(0, \xi_2) = x_2|_{\widehat{Q_4 Q_1}} \cdot \delta_{k0}, \quad \hat{x}_{2,k}(1, \xi_2) = x_2|_{\widehat{Q_3 Q_2}} \cdot \delta_{k0},$$

$$(3.7d) \quad \hat{x}_{2,k}(\xi_1, 0) = x_2|_{\widehat{Q_4 Q_3}} \cdot \delta_{k0}, \quad \hat{x}_{2,k}(\xi_1, 1) = \hat{s}_k(z),$$

where $\delta_{mn} = 0$ if $m \neq n$ and $\delta_{mn} = 1$ if $m = n$ is the Kronecker delta function. Solutions of the deterministic boundary value problems (3.6)–(3.7) give the stochastic mapping function $x_i(\xi, \omega)$ in (3.5), whose metrics terms and Jacobian can be readily evaluated.

3.3. Numerical solutions of the transformed equations. Since the stochastic mapping $x_i(\xi, \omega)$ in (2.2) is represented by (3.5) as a function of the random variables $\{Y_k(\omega)\}_{k=1}^K$, the metrics terms and the Jacobian corresponding to the coordinate transformation from x to ξ become functions of $\{Y_k(\omega)\}_{k=1}^K$ as well. In particular, the Jacobian takes the form

$$(3.8) \quad J(\xi, \omega) \equiv \frac{\partial(\xi_1, \dots, \xi_d)}{\partial(x_1, \dots, x_d)} = J(\xi, Y_1(\omega), \dots, Y_K(\omega)).$$

Hence, according to the Doob–Dynkin lemma [25], a solution of the SBVP (2.4) can be described by a finite number of random variables $\{Y_k(\omega)\}_{k=1}^K$, i.e.,

$$(3.9) \quad u(x, \omega) = u(x, Y_1(\omega), \dots, Y_K(\omega)).$$

The transformed SBVP (2.4) in the fixed domain E can be solved by a variety of techniques, including perturbation methods [18] and second-moment analyses [22]. In this paper, we use two complementary approaches, Monte Carlo simulations and stochastic Galerkin methods.

To facilitate numerical implementation, we further assume that the random variables $\{Y_k(\omega)\}_{k=1}^K$ are mutually independent, rather than just uncorrelated. (Such an assumption is not needed for Gaussian processes, for which independence and uncorrelation are equivalent.) While this assumption might introduce additional errors in the finite-term approximations (3.1) and (3.2) of target random processes, it enables one to define the corresponding Hilbert functional spaces via simple tensor product rules. In other words, the independence assumption is made for technical convenience, and has been employed in many applications in stochastic simulations, e.g., [3, 21, 36] and references therein. We also remark that similar assumptions are often made in sampling methods, where random number generators typically generate *independent*, not just uncorrelated, series of random numbers. It is worthwhile to point out that it is possible to construct multidimensional functional spaces based on a finite number of *dependent* random variables [31]. However, in its current form such a construction is not amenable to a straightforward numerical implementation.

3.3.1. Monte Carlo simulations. Monte Carlo simulations (MCS) are one of the most developed methods for solving stochastic differential equations. Although their convergence rate is relatively slow—a typical Monte Carlo simulation consisting of M realizations converges as $1/\sqrt{M}$ (see [11])—it is independent from the number of random variables $\{Y_k(\omega)\}_{k=1}^K$. We remark that the presence of random boundaries $\partial D(\omega)$ makes the direct use of MCS for solving the RDP (2.1) less than straightforward. Since each realization of the random domain $D(\omega_j), j = 1, \dots, M$, is different, a remeshing procedure is needed to render the statistical averaging of a solution at any point x in the domain meaningful.

In our approach, we apply MCS to the transformed SBVP (2.4) instead. Since this SBVP is defined on the fixed deterministic domain E , the use of MCS becomes straightforward and consists of the following steps:

1. for a given number of realizations M , generate the independent random variables $\{Y_k(\omega_j)\}_{k=1}^K$, for $j = 1, \dots, M$;
2. for each $j = 1, \dots, M$, use (3.1) and (3.2) to construct realizations of the random boundary $\widehat{Q_1 Q_2}(\omega_j) = r(\omega_j)\mathbf{e}_1 + s(\omega_j)\mathbf{e}_2$, and solve Laplace's equations (3.6)–(3.7) to obtain realizations of the stochastic mapping $x_i(\xi, \omega_j), i = 1, \dots, d$;
3. for each $j = 1, \dots, M$, evaluate the metrics terms and the Jacobian $J(\xi, \omega_j)$, and solve the SBVP (2.4) in the deterministic domain $\xi \in E \subset \mathbb{R}^d$;
4. postprocess the results to evaluate the solution's statistics, e.g., $\langle u(\xi) \rangle \equiv \mathbb{E}[u] = M^{-1} \sum_{j=1}^M u(\xi, \omega_j)$.

For each realization $j = 1, \dots, M$, step 3 solves a deterministic problem on a deterministic domain E , which can be accomplished with any suitable spatial discretization scheme.

3.3.2. Stochastic Galerkin method. Stochastic Galerkin (SG) methods are polynomial-type expansions in the random space. In general, these methods exhibit fast convergence rates, provided that solutions are sufficiently smooth in the random space. The first SG methods employed polynomial chaos expansions [14], which are based on the Wiener–Hermite expansion. More recent developments of the generalized polynomial chaos employ non-Hermite polynomials to improve efficiency for a wide class of problems. Such generalizations include global polynomial expansions based on hypergeometrical polynomials [37, 36, 38], piecewise polynomial expansions [3, 9], and wavelet basis expansions [20, 21]. Here we briefly review the framework based on global polynomial expansions.

Let $\{Y_i\}_{i=1}^K$ be independent random variables with probability density functions $\rho_i : \Gamma_i \rightarrow \mathbb{R}^+$, and assume that their images $\Gamma_i \equiv Y_i(\Omega)$ are bounded intervals in \mathbb{R} for $i = 1, \dots, K$. Then

$$(3.10) \quad \rho(y) = \prod_{i=1}^K \rho_i(Y_i) \quad \forall y \in \Gamma$$

is the joint probability density of $y = (Y_1, \dots, Y_K)$ with the support

$$(3.11) \quad \Gamma \equiv \prod_{i=1}^K \Gamma_i \subset \mathbb{R}^K.$$

This allows one to rewrite (2.4) as a $(d + K)$ -dimensional differential equation

$$(3.12) \quad \begin{aligned} \mathcal{L}(\xi, y; u) &= f(\xi, y), & (\xi, y) &\in E \times \Gamma, \\ \mathcal{B}(\xi, y; u) &= g(\xi, y), & (\xi, y) &\in \partial E \times \Gamma. \end{aligned}$$

Let us define a one-dimensional polynomial space in $L^2_{\rho_i}(\Gamma_i)$, the space for all square integrable functions in Γ_i with respect to measure $\rho_i dY_i$,

$$(3.13) \quad W_i^{p_i} \equiv \{v : \Gamma_i \rightarrow \mathbb{R} : v \in \text{span} \{\phi_m(Y_i)\}_{m=0}^{p_i}\}, \quad i = 1, \dots, K,$$

where $\{\phi_m(Y_i)\}$ form a set of orthogonal polynomials satisfying the orthogonality conditions

$$(3.14) \quad \int_{\Gamma_i} \rho_i(Y_i) \phi_m(Y_i) \phi_n(Y_i) dY_i = h_m^2 \delta_{mn},$$

with normalization factors $h_m^2 = \int_{\Gamma_i} \rho_i(Y_i) \phi_m^2(Y_i) dY_i$. Then, the corresponding K -dimensional polynomial space is defined by

$$(3.15) \quad W_{K,p} \equiv \bigotimes_{|\mathbf{p}| \leq p} W_i^{p_i},$$

where the tensor product is over all possible combinations of the multi-index $\mathbf{p} = (p_1, \dots, p_K) \in \mathbb{N}_0^K$ such that the length of the multi-index satisfies $|\mathbf{p}| = \sum_{k=1}^K p_k \leq p$. The total number of basis functions in (3.15) is $(K + p)! / (K! p!)$.

The type of orthogonal polynomials $\{\phi_m(Y_i)\}$ in (3.14) is determined by the probability density function of $Y_i(\omega)$, for $i = 1, \dots, K$. For example, uniform distributions are best approximated with Legendre polynomials, while Hermite polynomials are most appropriate for Gaussian distributions. A detailed list of such correspondences and the rates of their convergence can be found in [37, 36].

Finally, an SG formulation of (3.12) is as follows. For all $\xi \in \bar{E}$, find $u_p(\xi, y) \in W_{K,p}$ such that

$$(3.16) \quad \int_{\Gamma} \rho(y) \mathcal{L}(\xi, y; u_p) v(y) dy = \int_{\Gamma} \rho(y) f(\xi, y) v(y) d\mathbf{y} \quad \forall v(y) \in W_{K,p}, \xi \in E,$$

$$(3.17) \quad \int_{\Gamma} \rho(y) \mathcal{B}(\xi; u_p) v(y) dy = \int_{\Gamma} \rho(y) g(\xi, y) v(y) dy \quad \forall v(y) \in W_{K,p}, \xi \in \partial E.$$

The weak formulation (3.16)–(3.17) results in a set of deterministic problems in the fixed domain E and can be further discretized by any standard discretization technique, including finite elements and finite volumes. Construction of stochastic Sobolev spaces for stochastic diffusion equations is discussed in detail in [3]. For more implementation details and numerical examples, see [37, 36].

3.3.3. Selection of a numerical method. The dimensionality of the problem (3.12) is $d + K$, although only d dimensions involve differentiations. The total number K of random variables $\{Y_i\}_{i=1}^K$ that is needed to represent the random boundary $\partial D(\omega)$ by (3.1) and (3.2) with a given accuracy depends on, among other factors, the correlation length of $\partial D(\omega)$. Although one may choose different decomposition methods in (3.1) and (3.2), in general, the value of K increases when the correlation length becomes smaller.

SG methods converge with increased order of p . In fact, an exponential convergence has been proved for stochastic diffusion equations in [3] and shown numerically for various stochastic equations in [36, 37, 38]. However, when $K \gg 1$ is very large, the total number of expansion terms $(K + p)!/K!p!$ increases quickly, and this effectively reduces the convergence rate with respect to the number of expansion terms. In this case, it may be necessary to resort to MCS, as their convergence rate, $1/\sqrt{M}$, albeit slower, is asymptotically independent of the value of K .

Thus, for low to moderate values of K (less than 10), SG methods are preferred, and for large values of $K \gg 1$, the Monte Carlo method is preferred. However, if high accuracy of a stochastic solution is required, then SG methods can be more efficient even for relatively large values of K . (For example, see [35] for computations with $K = 38$ for a three-dimensional time-dependent heat transfer problem.)

4. Applications to elliptic equations in random domains. In this section, we apply the computational framework described above to elliptic problems in single- and double-connected random domains.

4.1. Formulation. Consider a deterministic Poisson equation with homogeneous Dirichlet boundary conditions in a random domain: for \mathcal{P} -a.e. $\omega \in \Omega$, $c, a : D(\omega) \rightarrow \mathbb{R}$, find $v : \bar{D}(\omega) \rightarrow \mathbb{R}$ such that

$$(4.1) \quad \begin{aligned} \nabla \cdot [c(x)\nabla v(x, \omega)] &= a(x) && \text{in } D(\omega), \\ v(x, \omega) &= 0 && \text{on } \partial D(\omega). \end{aligned}$$

The stochastic mapping (2.2) transforms (4.1) into a stochastic Poisson equation on a deterministic domain E : for \mathcal{P} -a.e. $\omega \in \Omega$, $\kappa, f, \alpha_{ij} : E \times \Omega \rightarrow \mathbb{R}$, $1 \leq i, j \leq d$, find $u : \bar{E} \times \Omega \rightarrow \mathbb{R}$ such that

$$(4.2) \quad \sum_{i=1}^d \frac{\partial}{\partial \xi_i} \left[\kappa(\xi, \omega) \sum_{j=1}^d \left(\alpha_{ij}(\xi, \omega) \frac{\partial u}{\partial \xi_j} \right) \right] = J^{-1} f(\xi, \omega) \quad \text{in } E,$$

$$u(\xi, \omega) = 0 \quad \text{on } \partial E,$$

where the random fields κ and f are the transformations of c and a , respectively; J is the transformation Jacobian defined in (3.8); and

$$(4.3) \quad \alpha_{ij}(\xi, \omega) = J^{-1} \nabla \xi_i \cdot \nabla \xi_j, \quad 1 \leq i, j \leq d.$$

The use of (3.1) and (3.2) to parameterize the random boundary $\partial D(\omega)$ with a finite number of random variables $\{Y_i(\omega)\}_{i=1}^K$ yields a strong form of (4.2),

$$(4.4) \quad \sum_{i=1}^d \frac{\partial}{\partial \xi_i} \left[\kappa(\xi, y) \sum_{j=1}^d \left(\alpha_{ij}(\xi, y) \frac{\partial u}{\partial \xi_j} \right) \right] = J^{-1} f(\xi, y) \quad \text{in } E \times \Gamma,$$

subject to the boundary condition

$$(4.5) \quad u(\xi, y) = 0 \quad \text{on } \partial E \times \Gamma.$$

In what follows, we solve the SBVP (4.4)–(4.5) by MCS and SG methods. Note that the left-hand side of (4.5) typically takes the form of a complicated function of the random vector y , even though the representation of the input, i.e., random boundary ∂D , is linear in y . Thus, in SG methods the projection of (4.5) onto the basis functions can be nontrivial. In this paper, we employ a typical approach that uses the quadrature/cubature rule with sufficient accuracy to ensure the accuracy of the projection (e.g., [37]).

4.2. Diffusion in a channel with a rough surface. Consider steady-state diffusion, described by (4.1) with $f \equiv 0$, in a two-dimensional channel $D(\omega) = \{(x_1, x_2) | 0 \leq x_1 \leq L_x, s(x_1, \omega) \leq x_2 \leq L_y\}$. To be specific, we set $L_x = 5$, $L_y = 1$, and treat the rough bottom boundary as a random field $s = s(x_1, \omega)$ with zero mean $\langle s(x_1, \omega) \rangle = 0$ and an exponential two-point covariance function

$$(4.6) \quad C_S(x_1, z_1) = \mathbb{E}[s(x_1, \omega)s(z_1, \omega)] = \exp\left(-\frac{|x_1 - z_1|}{b}\right),$$

where $b > 0$ is the correlation length. In the computational examples below, $b = L_x/5 = 1$, which corresponds to a boundary of moderate roughness. Finally, we prescribe Dirichlet boundary conditions $u = 1$ at $x_2 = L_y$ and $u = 0$ elsewhere.

We employ the finite-term KL-type expansion (3.2) to decompose the boundary process. The expansion coefficients $\{\hat{s}_k\}_{k=1}^K$ are given by $\hat{s}_k(x_1) = \sqrt{\lambda_k}\psi_k(x_1)$, where $\{\lambda_k, \psi_k(x_1)\}$ are the eigenvalues and eigenfunctions of the integral equations

$$(4.7) \quad \int C_S(x_1, z_1)\psi_k(z_1)dz_1 = \lambda_k\psi_k(x_1), \quad k = 1, \dots, K.$$

Then the decomposition (3.2) becomes

$$(4.8) \quad s(x_1, \omega) \approx \sigma \sum_{k=1}^K \hat{s}_k(x_1)Y_k(\omega) = \sigma \sum_{k=1}^K \sqrt{\lambda_k}\psi_k(x_1)Y_k(\omega).$$

We set $\{Y_i(\omega)\} \sim U(-1, 1)$ to be independent uniform random variables in $(-1, 1)$ and use the parameter $0 < \sigma < 1$ to control the maximum deviation of the rough surface. (In the computational examples in this section, we set $\sigma = 0.1$.) We employ Legendre polynomials as the basis functions (3.13) in the SG method, since they form the optimal basis corresponding to uniform random inputs [37].

It is worthwhile to stress again that the expansion (4.8) introduces two sources of errors—the errors due to the finite K -term truncation and the errors due to the assumption of independence of $\{Y_k(\omega)\}$. The truncation error is typically controlled by selecting the value of K to ensure that the eigenvalues $\{\lambda_k\}$ with $k > K$ are sufficiently small. For example, our numerical tests reveal that the expansion (4.8) with $K = 10$ captures 95% of the L_2 norm. Hence, we employ a ten-term KL expansion to represent the random boundary, and show some realizations of the boundary in Figure 4.1(a). Theoretical error estimates of such truncations can be found in [12]. Error analysis on the independence assumption is lacking and lies outside the scope of the present study.

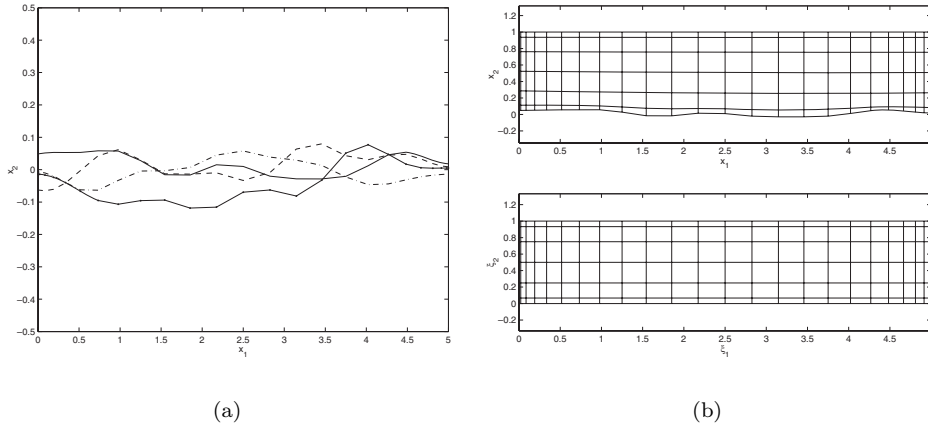


FIG. 4.1. Channels with a rough wall generated with the ten-term ($K = 10$) KL expansion (4.8). (a) Four sample realizations of the bottom boundary $s(x_1, \omega_j)$ ($j = 1, \dots, 4$). (b) A sample realization of the channel in the physical domain (x_1, x_2) and in the mapped domain in (ξ_1, ξ_2) . Chebyshev meshes are used in both domains.

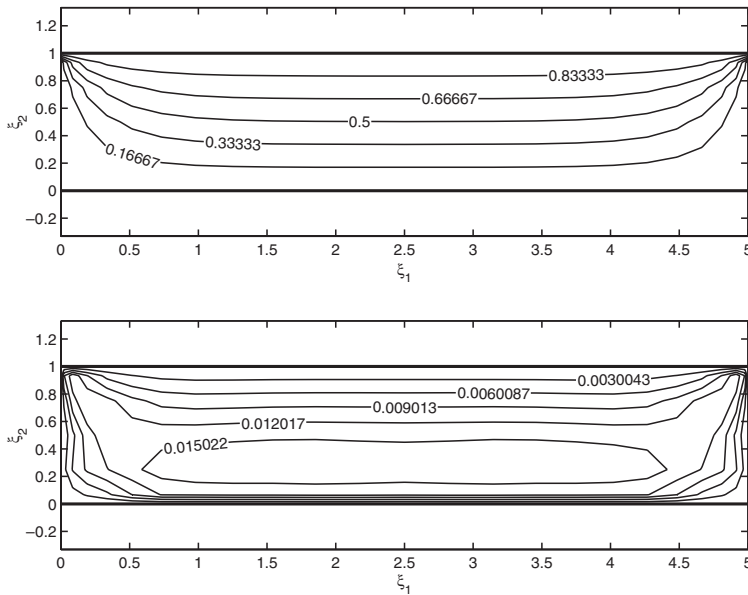


FIG. 4.2. The mean and STD of the dependent variable u , computed with the SG method.

Figure 4.1(b) shows a realization of the channel $D(\omega_j)$ mapped onto the corresponding rectangular domain $E = [0, L_x] \times [0, L_y]$. The mapping Laplace equations (3.3) are solved by the Chebyshev collocation method. Figure 4.1(b) also shows the Chebyshev collocation mesh points in both the physical domain D and the mapped domain E .

The stochastic elliptic problem (4.2) is solved in the mapped rectangular domain E with the SG method described in section 3.3.2. The Chebyshev collocation method is used in both ξ_1 and ξ_2 directions. Figure 4.2 shows the first two ensemble moments of the solution, i.e., its mean (top) and standard deviation (STD) (bottom). We

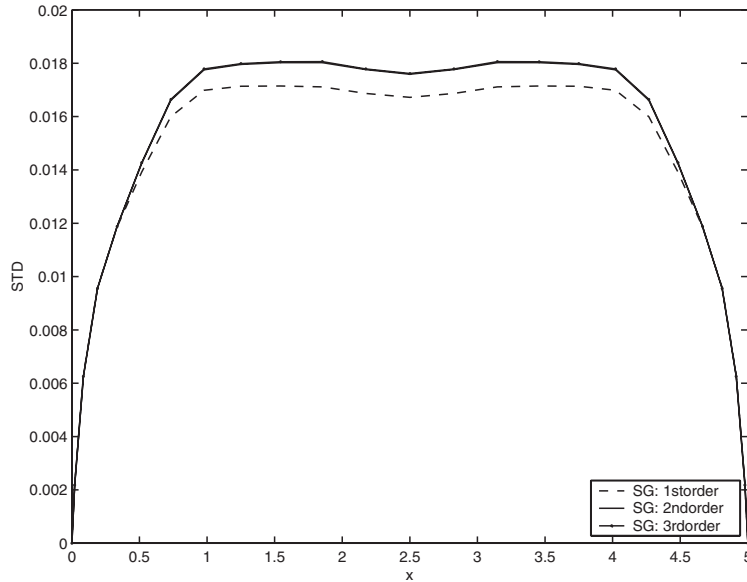


FIG. 4.3. The STD profiles along the cross section $y = 0.25$, computed with the first-, second-, and third-degree Legendre polynomials.

observe that the STD reaches its maximum close to, but not at, the random bottom boundary.

To ascertain the convergence of the polynomial chaos expansion, we examine the STD profile along the cross section $y = 0.25$, where the STD is close to its maximum. Figure 4.3 shows the STD profiles obtained with different orders of Legendre expansions. One can see that the second order is sufficient for the Legendre expansion to converge. Although not shown here, the convergence of the mean solution is similar to that of the STD.

MCS are also conducted to verify the results obtained by the SG method. Figure 4.4 compares the STD profile along the cross section $y = 0.25$ computed via the second-order Legendre expansion with those obtained from MCS. We observe that as the number of realizations increases, the MCS results converge to the converged SG results. With about 2,000 realizations, the MCS results agree well with SG results. In this case, at second order ($p = 2$) and ten random dimensions ($K = 10$), the SG method requires $(K + p)!/K!p! = 66$ basis functions and is computationally more efficient than MCS. In CPU time, the second-order SG method is approximately 20 times faster than MCS with 2,000 realizations.

4.3. Diffusion in double-connected domains with rough exclusion. Consider steady-state diffusion, described by (4.1) with $f \equiv 0$, in a double-connected domain $D(\omega)$ consisting of the square $[-2, 2] \times [-2, 2]$ with a randomly perturbed unit circular exclusion. A sample realization of such a domain is shown in Figure 4.5(a), and several sample realizations of the surface of the random exclusion are depicted in Figure 4.5(b). The boundary conditions are $u = 1$ along the surface of the exclusion and $u = 0$ along the outer square.

The inner random boundary is constructed and parameterized by superimposing a zero-mean random perturbation process on the radius $R(\theta)$ of a unit circle centered

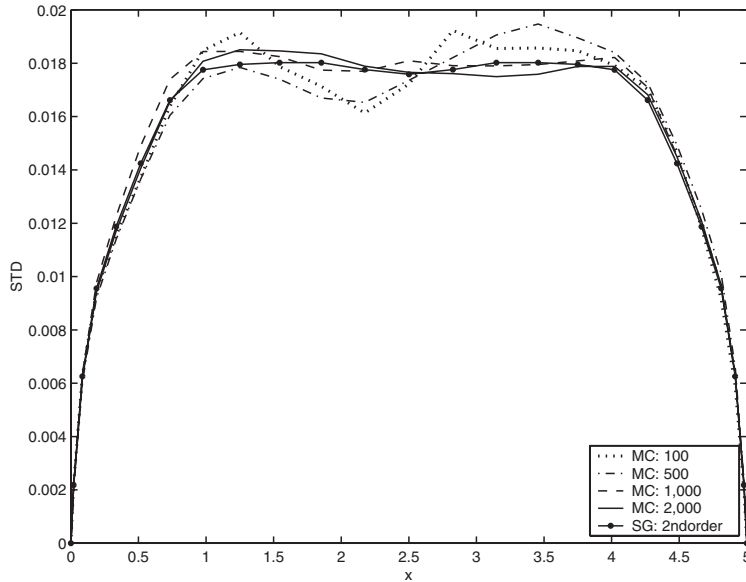


FIG. 4.4. The STD profiles along the cross section $y = 0.25$, computed with the SG method (the second-order Legendre chaos) and the MCS consisting of 100, 500, 1,000, and 2,000 realizations.

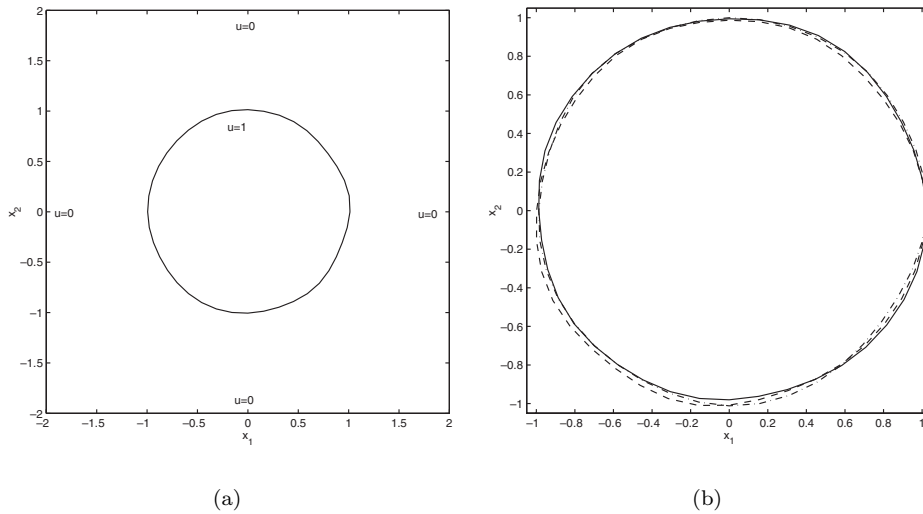


FIG. 4.5. A double-connected domain with a rough circular exclusion generated with the 16-term ($N = 16$) Fourier expansion (4.9). (a) A sample realization of the random computational domain. (b) Three sample realizations of the circular exclusion $R(\theta, \omega_j)$ ($j = 1, \dots, 4$).

at $(0, 0)$, where $0 \leq \theta \leq 2\pi$. In other words, the inner boundary is defined as $(x_1, x_2) = (R \cos \theta, R \sin \theta)$, for $0 \leq \theta \leq 2\pi$, where $R(\theta, \omega) = 1 + \sigma R'(\theta, \omega)$ is the radius. Here $0 < \sigma < 1$ is used to control the maximum deviation of the process. We require that both $\langle R' \rangle = 0$ and the statistics of $R(\theta, \omega)$ be *rotationally invariant* on the circle, i.e., that $\langle R'(\theta_1)R'(\theta_2) \rangle = C_R(|\theta_1 - \theta_2|)$.

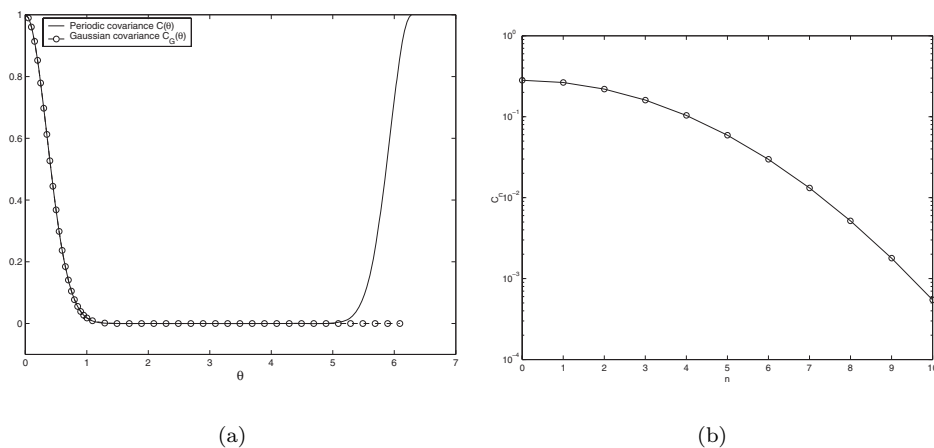


FIG. 4.6. (a) Periodic covariance function $C(\theta)$ (solid line) based on the nonperiodic Gaussian function $C_G = \exp(-\theta^2/b^2)$ with $b = 0.5$ (dashed line with circles). (b) Decay of the Fourier cosine coefficients of the periodic covariance function.

Since the random process $R'(\theta, \omega)$ is periodic, we use a Fourier-type expansion

$$(4.9) \quad R'(\theta, \omega) = \sum_{n=-N}^N R_n(\omega) e^{-in\theta}$$

for its decomposition into a finite number of random variables (see (3.1) and (3.2)). In this expansion, the coefficients $R_n(\omega) = R_n^r(\omega) + iR_n^i(\omega)$ are complex random variables. It is straightforward to show that if R_n^r and R_n^i are statistically independent for all n , and have zero mean and the variance of $C_n/4$, where $C_n = \frac{1}{\pi} \int_0^{2\pi} C_R \cos(n\theta) d\theta$ are the coefficients of the Fourier cosine series of the covariance function C_R , then the random field $R'(\theta, \omega)$ given by (4.9) has the prescribed covariance function C_R . (It is worth noting that in periodic domains, Fourier expansion is in fact the KL expansion.)

A periodic covariance function $C_R(|\theta_1 - \theta_2|)$ with the period of 2π is constructed by extending the standard Gaussian covariance function $C_G = \exp(-(\theta_1 - \theta_2)^2/b^2)$ to the periodic domain $(0, 2\pi)$, where b is the correlation length. Figure 4.6(a) shows such a periodic covariance function and contrasts it with the standard nonperiodic Gaussian covariance function. Figure 4.6(b) demonstrates the decay of the Fourier cosine coefficients $\{C_n\}$ for the periodic covariance function with the correlation length $b = 0.5$. Based on the decay of C_n , we choose $N = 8$ ($C_9 = 0.0052$, $C_1 = 0.2821$, $C_9/C_1 < 2\%$).

In the following examples, we set the coefficients $R_n^r, R_n^i, n = 1, \dots, N$, in the expansion (4.9) to be independent uniform random variables of $U(-1, 1)$. This results in a 16-dimensional ($K = 2N = 16$) random space Γ for problem (4.2). In the computational examples below, we set $\sigma = 0.02$. We again use Legendre expansion in the SG method to represent the uniform random inputs.

To map the double-connected random domain $D(\omega)$ onto a single-connected deterministic domain E , we introduce an artificial cut in the domain D , as shown in Figure 4.7. This cut dissects the overall boundary into four segments: the inner boundary \overline{AB} , the cut \overline{BC} , the outer boundary \overline{CD} , and the cut \overline{DA} . Note that the segments \overline{BC} and \overline{AD} are at the same physical locations, although while solving the

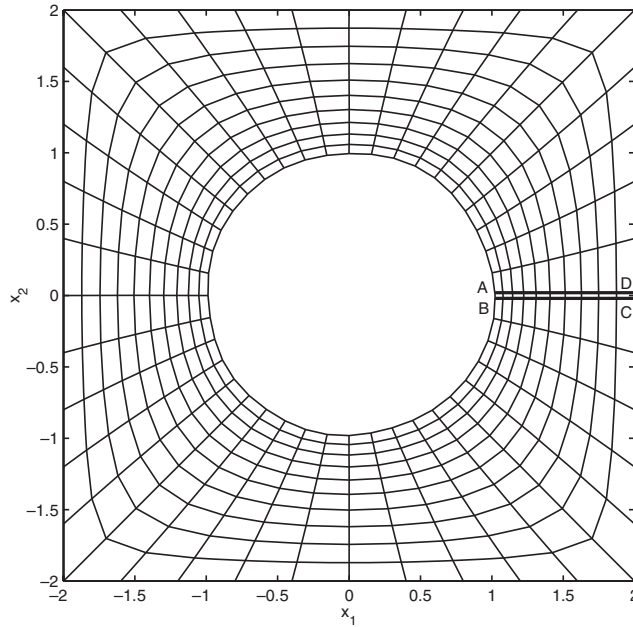


FIG. 4.7. Random double-connected domain constructed with the 16-term ($N = 2K = 16$) Fourier expansion, and the corresponding computational mesh.

Laplace equations (3.3) they are treated as two distinct boundaries. To emphasize this point, these two cuts are shown as two separate lines in Figure 4.7.

The mapped domain in (ξ_1, ξ_2) is a rectangle of $ABCD$, whose length \overline{AB} and \overline{CD} is 2π and width \overline{BC} and \overline{DA} is 1. To solve (3.6), we use the Fourier collocation method in the ξ_1 -direction (because of the periodicity) and the second-order finite difference method in the ξ_2 -direction. Figure 4.7 shows a sample resulting mesh in (x_1, x_2) .

The mapped stochastic Poisson equation (4.2) is solved with the 40-point Fourier collocation scheme in the ξ_1 -direction, and the ten-point second-order finite difference scheme in the ξ_2 -direction. (Numerical tests have been conducted to ensure resolution independence of the solutions in the physical domain.) The resulting mean and standard deviation of the solution are shown in Figure 4.8. Note that in the construction of the inner boundary, the dominating mode ($n = 1$) in the Fourier expansion (4.9) has a period of 2π (the $\sin \theta$ and $\cos \theta$ modes). This results in the two local extrema in the standard deviation field.

These numerical solutions are compared with those obtained from MCS. Figure 4.9 compares the STD profiles obtained with both methods along the radius of $R \approx 1.21$. Due to the smallness of the random input ($\sigma = 0.02$), both MCS and the SG method converge quickly. In fact, the solutions (mean and STD) obtained with the first- and second-order Legendre-chaos expansions almost completely coincide. Also, we observe the convergence of the Monte Carlo method as the number of realizations increases. This example has 16 dimensions in random space ($K = 16$). At first order ($p = 1$), the SG method needs $(K + p)!/K!p! = 17$ terms, and is more efficient than the Monte Carlo method.

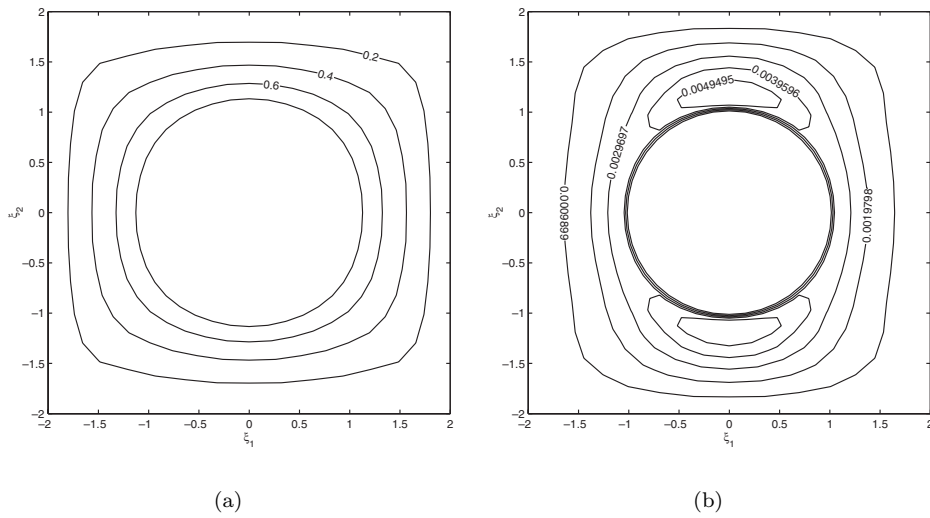


FIG. 4.8. (a) The mean $\langle u(x) \rangle$ and (b) STD $\sigma_u(x)$ of the random state variable $u(x, \omega)$, computed with the SG method.

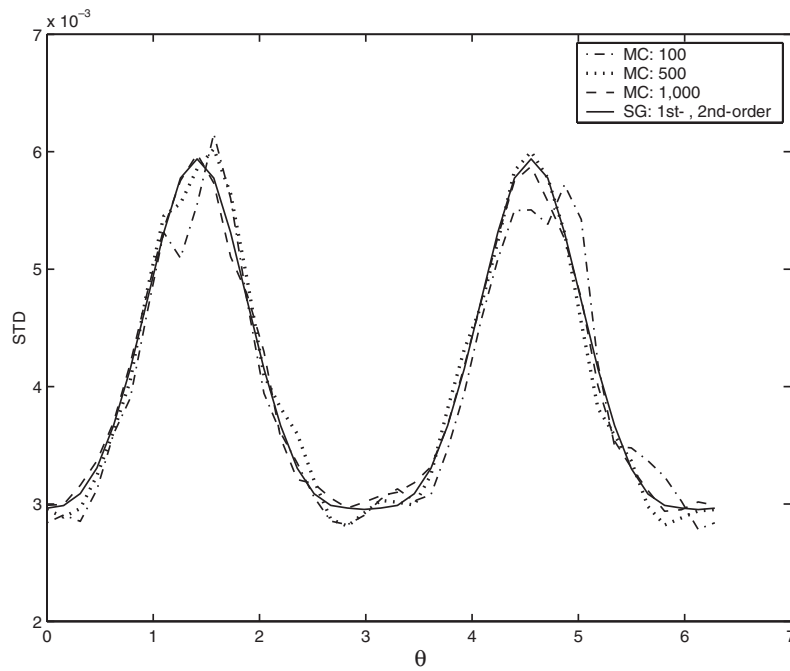


FIG. 4.9. The STD profiles along the radial cross section $R = 1.21$, computed with the SG method (the first- and second-order Legendre chaos) and the MCS consisting of 100, 500, and 1,000 realizations.

5. Summary. We have proposed a computational framework for the computation of deterministic/stochastic differential equations defined on *random domains*. A key component of the proposed approach is the use of stochastic mappings to transform the original problem into a (better understood) problem of stochastic equations in *deterministic domains*. While a variety of such stochastic mappings can be designed, here we have implemented a mapping defined by solutions of the Laplace equations. We have used numerical examples involving single-connected and double-connected random domains to demonstrate the versatility of the mapping technique.

This random mapping enables us to apply the existing analytical/numerical methods for the resulting transformed stochastic equations in fixed domains. In random spaces, we have presented methods based on Monte Carlo simulations and stochastic Galerkin methods, although we emphasize that other suitable techniques can be used. In physical spaces, we have used a variety of discretizational methods, including the Chebyshev collocation method, Fourier collocation method, and finite difference method. We applied our approach to the elliptic problems in the single- and double-connected random domains, and examined the convergence and efficiency of MCS and SG methods.

Several issues need to be addressed:

- *Error estimates.* There are several sources of errors, in addition to the discretizational errors in solving the transformed SBVP (2.4). In particular, the errors in solving the mapping problems (3.3) and their effect on the Jacobian evaluation (3.8) and the solution of SBVP (2.4) are important. Also, the accurate approximation of the random processes defining rough boundaries by a finite number of random variables in (3.1) and (3.2) plays a key role in the proposed approach. This by itself is an active research area. Furthermore, the effect of the representation errors on the overall accuracy of the present approach is unclear. For example, for an elliptic equation, a small error in the approximation of the shape of a Neumann boundary may be magnified in the final solution [1]. Hence a complete error analysis of the proposed method is required, in addition to the error analysis of the boundary representation.
- *The well-posedness of problems with random geometries.* We have assumed that the random boundary $\partial D(\omega)$ is sufficiently regular for the RDP (2.1) to be well-posed. For example, for the elliptic problems considered in section 4, the *precise* regularity requirements on the boundary $\partial D(\omega)$ to guarantee the well-posedness, e.g., coercivity, of the transformed stochastic elliptic equation (4.2) is unclear. We thus have restricted ourselves to domains with random boundaries of low to moderate roughness in the numerical examples. The rigorous regularity requirements of the boundary are problem-specific and remain an open issue for a wide class of important problems.
- *Domain decompositions and hybrid methods.* In many cases, the transformed stochastic equations are expected to be more complicated than their original counterparts (compare, for example, (4.1) and (4.2)). However, such transformed equations need to be solved only in the region close to the random boundary. Figure 5.1 shows a schematic of the decomposition of the computational domain into a “boundary region” and a “far-field region,” in which the transformed and original equations, respectively, are to be solved. These two equations are coupled through random boundary conditions on the interface between the two domains.

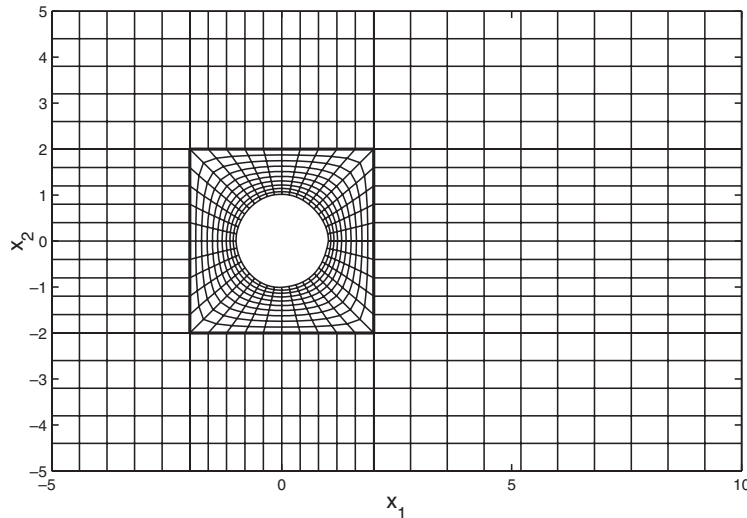


FIG. 5.1. Schematic representation of a computational mesh for a double-connected domain with a random inclusion. The interface between the “boundary region” and “far-field region” is shown in bold.

REFERENCES

- [1] I. BABUŠKA AND J. CHLEBOUN, *Effects of uncertainties in the domain on the solution of Neumann boundary value problems in two spatial dimensions.*, Math. Comput., 71 (2002), pp. 1339–1370.
- [2] I. BABUŠKA AND J. CHLEBOUN, *Effects of uncertainties in the domain on the solution of Dirichlet boundary value problems*, Numer. Math., 93 (2003), pp. 583–610.
- [3] I. BABUŠKA, R. TEMPONE, AND G. E. ZOURARIS, *Galerkin finite element approximations of stochastic elliptic differential equations*, SIAM J. Numer. Anal., 42 (2004), pp. 800–825.
- [4] D. BEGIS AND R. GLOWINSKI, *Application de la méthode des éléments finis à l’approximation d’un problème de domaine optimal. Méthode de résolution des problèmes approchés*, Appl. Math. Optim., 2 (1975), pp. 130–169.
- [5] A. BEJAN, *Shape and Structure, from Engineering to Nature*, Cambridge University Press, New York, 2000.
- [6] M. BLYTH AND C. POZRIKIDIS, *Heat conduction across irregular and fractal-like surfaces.*, Int. J. Heat Mass Transf., 46 (2003), pp. 1329–1339.
- [7] M. BRADY AND C. POZRIKIDIS, *Diffusive transport across irregular and fractal walls.*, Proc. R. Soc. Lond. A Math. Phys. Sci., 442 (1993), pp. 571–583.
- [8] D. CAJUEIRO, V. SAMPAIO, C. DE CASTILHO, AND R. ANDRADE, *Fractal properties of equipotentials close to a rough conducting surface*, J. Phys. Condensed Matter, 11 (1999), pp. 4985–4992.
- [9] M. DEB, I. BABUŠKA, AND J. ODEN, *Solution of stochastic partial differential equations using Galerkin finite element techniques*, Comput. Methods Appl. Mech. Engrg., 190 (2001), pp. 6359–6372.
- [10] C. EVERTSZ AND B. MANDELBROT, *Harmonic measure around a linearly self-similar tree*, J. Phys. A, 25 (1992), pp. 1781–1797.
- [11] G. FISHMAN, *Monte Carlo: Concepts, Algorithms, and Applications*, Springer-Verlag, New York, 1996.
- [12] P. FRAUENFELDER, C. SCHWAB, AND R. TODOR, *Finite elements for elliptic problems with stochastic coefficients*, Comput. Methods Appl. Mech. Engrg., 194 (2005), pp. 205–228.
- [13] M. FYRILLAS AND C. POZRIKIDIS, *Conductive heat transport across rough surfaces and interfaces between two conforming media*, Int. J. Heat Mass Transf., 44 (2001), pp. 1789–1801.
- [14] R. GHANEM AND P. SPANOS, *Stochastic Finite Elements: A Spectral Approach*, Springer-Verlag, New York, 1991.
- [15] J. GREENWOOD AND J. WILLIAMSON, *Contact of nominally flat surfaces*, Proc. Roy. Soc. A, 295 (1966), pp. 300–319.

- [16] M. GRIGORIU, *Simulation of stationary non-Gaussian translation processes*, J. Eng. Mech., 124 (1998), pp. 121–126.
- [17] H. HOMEIER AND D. KINGHAM, *Effects of local field variations on the contrast of a field-ion microscope*, J. Phys. D, 16 (1983), pp. L115–L120.
- [18] M. KLEIBER AND T. HIEN, *The Stochastic Finite Element Method*, John Wiley, New York, 1992.
- [19] Y. N. LAZAREV, P. V. PETROV, AND D. M. TARTAKOVSKY, *Interface dynamics in randomly heterogeneous porous media*, Adv. Water Resour., 28 (2005), pp. 393–403.
- [20] O. LE MAITRE, O. KNIO, H. NAJM, AND R. GHANEM, *Uncertainty propagation using Wiener-Haar expansions*, J. Comput. Phys., 197 (2004), pp. 28–57.
- [21] O. LE MAITRE, H. NAJM, R. GHANEM, AND O. KNIO, *Multi-resolution analysis of Wiener-type uncertainty propagation schemes*, J. Comput. Phys., 197 (2004), pp. 502–531.
- [22] W. LIU, T. BELYTSCHKO, AND A. MANI, *Probabilistic finite elements for nonlinear structural dynamics*, Comput. Methods Appl. Mech. Engrg., 56 (1986), pp. 61–81.
- [23] M. LOËVE, *Probability Theory*, 4th ed., Springer-Verlag, New York, Berlin, 1977.
- [24] M. MILLER, A. CEREZO, M. HETHERINGTON, AND G. SMITH, *Atom Probe Field Ion Microscopy*, Monographs on the Physics and Chemistry of Materials, Oxford University Press, Oxford, UK, 1996.
- [25] B. ØKSENDAL, *Stochastic Differential Equations. An Introduction with Applications*, 5th ed., Springer-Verlag, Berlin, 1998.
- [26] S. RICHARDSON, *A model for the boundary condition of a porous material, Part 2*, J. Fluid Mech., 49 (1971), pp. 327–336.
- [27] J. RUDZITIS, V. PADAMANS, E. BORDO, AND R. HAYTHAM, *Random process model of rough surfaces contact*, Meas. Sci. Technol., 9 (1998), pp. 1093–1097.
- [28] S. SAKAMOTO AND R. GHANEM, *Simulation of multi-dimensional non-Gaussian non-stationary random fields*, Prob. Eng. Mech., 17 (2002), pp. 167–176.
- [29] K. SARKAR AND C. MENEVEAU, *Gradients of potential fields on rough surfaces: Perturbative calculation of the singularity distribution function $f(\alpha)$ for small surface dimension*, Phys. Rev. E, 47 (1993), pp. 95–966.
- [30] M. SHINOZUKA AND G. DEODATIS, *Simulation of stochastic processes by spectral representations*, Appl. Mech. Rev., 44 (1991), pp. 191–203.
- [31] C. SOIZE AND R. GHANEM, *Physical systems with random uncertainties: Chaos representations with arbitrary probability measure*, SIAM. J. Sci. Comput., 26 (2004), pp. 395–410.
- [32] G. TAYLOR, *A model for the boundary condition of a porous material, Part 1*, J. Fluid Mech., 49 (1971), pp. 319–326.
- [33] J. THOMPSON, Z. WARSI, AND C. MASTIN, *Numerical Grid Generation*, Elsevier Science, Amsterdam, 1985.
- [34] M. VIGNES-ADLER, P. ADLER, AND P. GOUGAT, *Transport processes along fractals. The Cantor-Taylor brush*, Physicochem. Hydrodynam., 8 (1987), pp. 401–422.
- [35] X. WAN, D. XIU, AND G. E. KARNIADAKIS, *Modeling uncertainty in three-dimensional heat transfer problems*, in Advanced Computational Methods in Heat Transfer VIII, Proceedings of the Eighth International Conference on Advanced Computational Methods in Heat Transfer, Lisbon, Portugal, 2004, B. Sunden, C. Brebbia, and A. Mendes, eds., WIT Press, Southampton, UK, 2004, pp. 15–24.
- [36] D. XIU AND G. E. KARNIADAKIS, *Modeling uncertainty in steady state diffusion problems via generalized polynomial chaos*, Comput. Methods Appl. Math. Engrg., 191 (2002), pp. 4927–4948.
- [37] D. XIU AND G. E. KARNIADAKIS, *The Wiener-Askey polynomial chaos for stochastic differential equations*, SIAM J. Sci. Comput., 24 (2002), pp. 619–644.
- [38] D. XIU AND G. E. KARNIADAKIS, *Modeling uncertainty in flow simulations via generalized polynomial chaos*, J. Comput. Phys., 187 (2003), pp. 137–167.
- [39] F. YAMAZAKI AND M. SHINOZUKA, *Digital generation of non-Gaussian stochastic fields*, J. Eng. Mech., 114 (1988), pp. 1183–1197.